Jordan Journal of Civil Engineering, Volume **11**, No. **3**, **2017**

Numerical Determination of End Bearing Capacity of Drilled Shafts in Sand

Ali Hasanzadeh [1)*] ***and Issa Shooshpasha*** [2)]

[1)] Ph.D. Student, Department of Civil Engineering, Babol Noshirvani University of Technology, P. O. Box 484, Babol, Iran.
[2)] Associate Professor, Department of Civil Engineering, Babol Noshirvani University of Technology, P. O. Box 484, Babol, Iran.
* Corresponding Author. E-Mail: a_hasanzade64@yahoo.com

ABSTRACT

Determination of axial capacity of piles has been a challenging problem since the beginning of the geotechnical engineering profession. The axial capacity of a single pile can be estimated by summing the skin friction capacity and the bearing capacity of the pile toe. In this paper, an attempt is made to numerically analyze the end bearing capacity of drilled shafts in sand. The numerical results obtained were compared with the results of pile load test. The comparison between numerical and experimental base load-settlement curves showed that the proposed numerical analysis produces satisfactory predictions. Then, variations of the end bearing capacity of drilled shafts *versus* embedment depth and pile diameter were studied. Numerical results showed that with the increase in embedment depth and pile diameter, the end bearing capacity increases, but with a decreasing rate. Moreover, the range of failure zone surrounding the pile tip is discussed.

KEYWORDS: Drilled shaft, Numerical analysis, End bearing capacity, Sand.

INTRODUCTION

Pile foundations are frequently used to support various structures built on sand/clay soils, where shallow foundations would undergo excessive settlements or shear failure (Ghashghaee Zadeh and Kalantari, 2011). Pile foundations can transfer the applied loads from the structure through the upper level strata to the bearing ground located at some depth below ground surface. Drilled shafts are a common type of pile foundations broadly described as cylindrical, deep, cast-in-place concrete foundations poured in and formed by a bored excavation. Drilled shaft is a versatile foundation system that has many advantages in comparison with other types of pile foundations. For example, the construction of drilled shafts generates less noise and vibration or, in many cases, a large diameter drilled shaft can replace a group of piles which in turn eliminates the need for a pile cap. Due to the flexural strength of a large diameter column of reinforced concrete, drilled shafts have enjoyed increased use for highway bridges in seismically active areas. In addition, drilled shafts may be used as foundations for other applications, such as retaining walls, sound walls or high mast lighting, where a simple support for overturning loads is the primary function of the foundation (Brown et al., 2010).

Pile foundation design, due to the complexity of the interaction mechanism between soil and pile, is still considered as one of the most difficult tasks in geotechnical engineering (Ai and Cheng, 2013). Bearing capacity is considered one of the significant factors that govern the design of pile foundations (Alkroosh and

Received on 22/11/2015.
Accepted for Publication on 15/5/2017.

Nikraz, 2012). The bearing capacity of piles is governed both by its structural strength and the supporting soil properties. Obviously, the smaller of the two values should be used for the design. Usually, the pile capacity based on soil properties governs the design except probably in timber piles (Kameswara Rao, 2011). The capacity of drilled shafts comes mainly from skin friction and end bearing. The skin friction develops between the shaft concrete and the surrounding soil. The skin friction is transmitted to the soil along the length of drilled shaft. However, the end bearing is analogous to shallow foundation bearing capacity with a very large depth of footing (Gunaratne, 2006). The end bearing capacity is transmitted to the base of drilled shaft. The end bearing capacity of drilled shafts, particularly in sandy soils, can have an important role in their design. In some projects, drilled shafts are designed primarily based on the magnitude of the end bearing capacity (Winterkorn and Fang, 1975). The end bearing capacity of drilled shafts can be estimated by static analysis, dynamic analysis, dynamic testing, *in situ* testing and pile load test. Several investigations have been conducted for the determination of end bearing capacity of piles (Dung et al., 2007; Ishihara 2010; Dung et al., 2011; Veiskarami et al., 2011; Manandhar and Yasufuku, 2012; Yu and Yang, 2012). On the other hand, the acceptance of numerical analyses in geotechnical problems is growing and finite element calculations are more and more used in the design of foundations. In this study, a modeling procedure is carried out to numerically determine the end bearing capacity of drilled shafts in sand. The obtained numerical prediction of end bearing capacity of drilled shafts is compared with the results of pile load test. The effects of embedment depth and pile diameter on the end bearing capacity are also discussed. Moreover, the range of failure zone around the pile tip is calculated.

Numerical Modeling

Numerical modeling was performed by using the Plaxis program. Plaxis is a two-dimensional (2-D) finite element computer program which is commercially available to analyze deformation and stability of various geotechnical problems. The program can be used in plane strain as well as in axisymmetric modeling. In this study, a numerical methodology is presented to model and simulate the end bearing capacity of drilled shafts in sandy soils. The Mohr-Coulomb elasto-plastic model has been applied in the modeling. Since cylindrical types of drilled shafts with constant circular cross-section have been routinely adopted in practice and the axial end bearing capacity of these drilled shafts has symmetry about the vertical axis, the axisymmetric option is used for this three-dimensional problem. In addition, the axisymmetric option decreases the number of elements in the solution procedure. In Figure 1, the hollow space

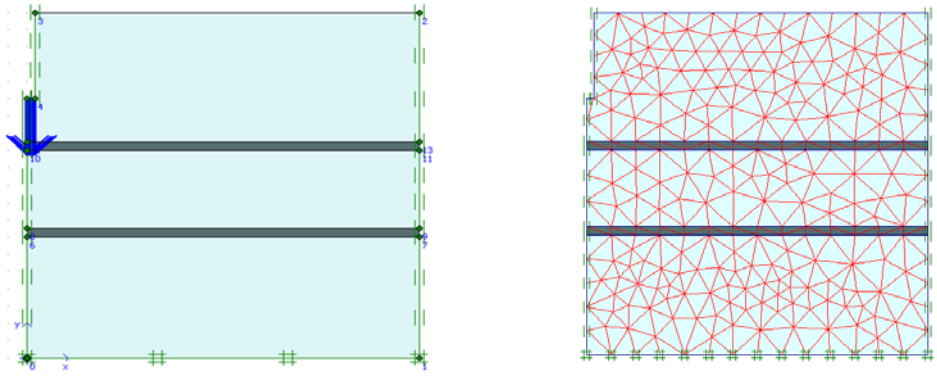

(a) (b)

Figure (1): (a) Numerical modeling of a drilled shaft; (b) The typical finite element mesh used in the study

on the top left side shows the location of the drilled shaft. The side and bottom boundaries are located far enough from the drilled shaft, so that the effects of boundaries on the response of drilled shaft would be negligible. The side boundaries are restricted in the horizontal direction and the bottom boundary is restricted in both horizontal and vertical directions. A fine finite mesh was used with 15-node triangular elements for modeling. In this numerical procedure, pile tip is given the vertical downward displacement for determining the end bearing capacity (Figure 2 (a)). As expected, stresses around the drilled shaft start to increase during this downward displacement. This increase in stress would be higher for the pile tip (Figure 2 (b)). The increase in stress for pile tip is registered and, as a result, the end bearing capacity of drilled shafts can be determined.

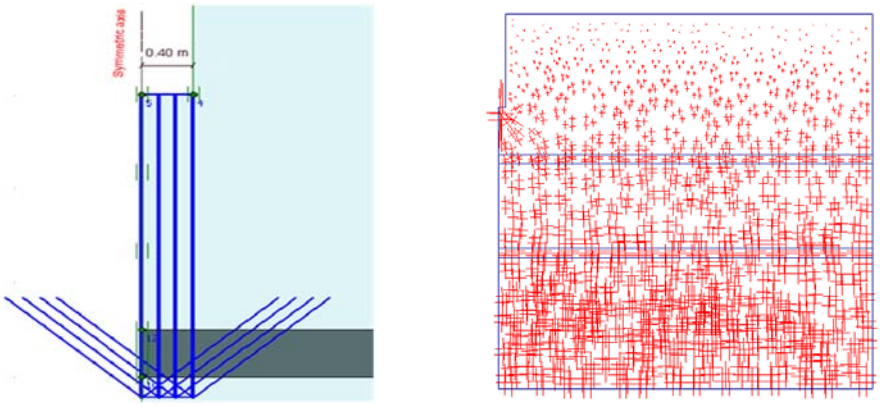

(a) (b)

Figure (2): (a) Close-up view of the tip of drilled shaft; (b) Stress distribution

Validation

Owing to uncertainties in geotechnical parameters, construction factors and other variables, the capacity of a drilled shaft often needs to be verified using a load test (Chen and Fang, 2009). Pile loading test results provide reliable data for engineers, that enable them to confirm and refine appropriate soil strength, stiffness and compressibility characteristics (Abdrabbo and Gaaver, 2013). Therefore, in order to evaluate the validity and performance of the proposed finite element analysis of pile base load-settlement response in sand, a load test on a drilled shaft is modeled and analyzed. To investigate the base load-settlement behavior of a single drilled shaft in sandy soil, a pile load test performed by the Georgia Institute of Technology (Mayne and Harris, 1993) is numerically modeled. The test site had a layer of residual, silty fine sand extending down to 19.5 m, underlain by partially weathered rock and then sound bedrock. A series of laboratory tests were performed on soil samples for the determination of basic soil properties. Grain size distribution analysis showed that soil consists of approximately 70% sand, with clay content of only about 8%. Moreover, the Atterberg limits testing showed that almost all of the soils were non-plastic. Table 1 depicts basic soil properties used in the analysis. The diameter of the drilled shaft was 76 cm with a length of 16.8 m. This pile load test was numerically modeled in the present study. The base load-settlement curve of pile load test (Mayne and Harris, 1993) and the modeled one are plotted together in Figure 3. The comparison depicts good agreement between the results.

Determination of End Bearing Capacity of Drilled Shafts (Case Study)

By performing a 20 m borehole in a region in Babolsar, north of Iran, soil stratigraphy has been recognized. Table 2 shows the soil stratigraphy. In Table

2, N, G_s and γ are: number of Standard Penetration Test (SPT) blows, specific gravity and unit weight of soil, respectively. These parameters are based on the results of laboratory and field tests. As seen, the soil consists of poorly-graded sand (SP) according to Unified Soil Classification System (USCS), except two 0.5-m layers that are of clay with low (CL) and high (CH) plasticity. The numerical modeling of a drilled shaft with an embedment depth of 5 m and a diameter of 80 cm in this site (in Babolsar) was previously shown (see Figure 1). In the numerical modeling, soil properties were assigned based on soil stratigraphy. The side boundaries, located at a horizontal distance of 20 m from the drilled shaft axis, are restricted in the horizontal direction and the bottom boundary, located at a vertical distance of 15 m from the end of the drilled shaft, is restricted in both horizontal and vertical directions. Pile tip is given the vertical downward displacement as shown in Figure 2. Figure 4 depicts the drilled shaft tip behavior in this site. As seen in Figure 4, with the increase in the downward displacement at the pile tip, the generated stresses at the pile tip also increase and no peak point is observed in the stress-settlement curve. So, it is essential to select a criterion for determining the ultimate end bearing capacity from the numerically obtained base load–settlement curve.

Table 1. Basic soil properties at Georgia Tech. site (Mayne and Harris, 1993)

Layer number	Depth (m)	Friction angle (˚)	Coefficient of lateral earth pressure at rest
1	0-1.82	34	0.44
2	1.82-3.93	34	0.44
3	3.93–5.93	37	0.40
4	5.93–7.93	33	0.46
5	7.93–9.93	32	0.47
6	9.93–11.93	32	0.47
7	11.93–13.93	36	0.41
8	13.93–14.93	38	0.38
9	14.93–16.76	36	0.41
10	16.76–18.28	36	0.41

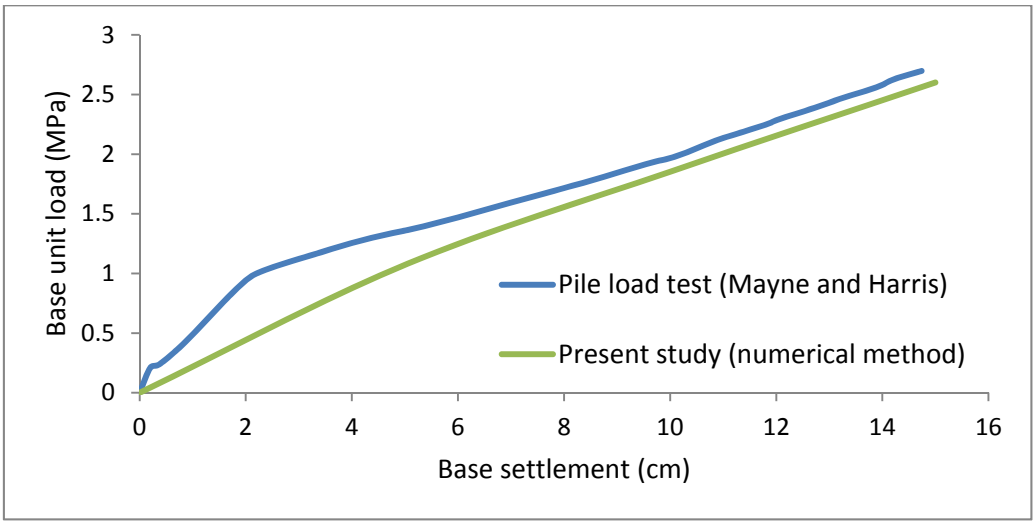

Figure (3): Comparison between base load-settlement curves obtained by pile load test and the present study

To assess the end bearing capacity of drilled shafts, researchers have suggested that the fully mobilized end bearing is the capacity that can be developed at a given displacement of the pile tip. Reese and Wright (1977) and O'Neill and Reese (1999) proposed that the required displacement for full mobilization of end bearing capacity is 5% D, where D is the shaft diameter. This value, according to Fleming et al. (1985) is 5–10% D. According to Coduto (2001) and White and Bolton (2005), the required pile tip displacement is 10% D. In addition, the suggested value by Tomlinson (1994) is 10–20% D. It should be noted that pile design based on selecting a pile tip displacement of more than 10% D may not satisfy the required serviceability condition of a structure. So, in this study, it is assumed that the end bearing capacity is mobilized at a tip displacement of 10% D. Therefore, the end bearing capacity of this drilled shaft at the tip displacement of 8 cm is registered, which is 836 kPa (see Figure 4).

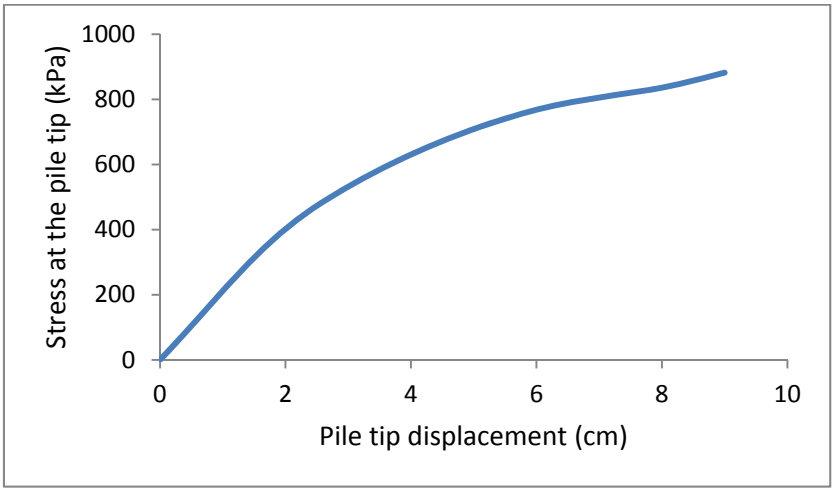

Figure (4): Tip stress *versus* tip displacement for a drilled shaft (embedment depth = 5 m, diameter = 80 cm)

Effect of Pile Embedment Depth

By conducting a series of numerical analyses for drilled shafts with embedment depths of 10 m and 15 m, the effect of embedment depth on the end bearing capacity of drilled shafts is investigated. The selected shaft diameter (D) in these analyses is a constant value of 80 cm. The results of analyses show that the end bearing capacity values of drilled shafts with embedment depths of 5, 10 and 15m are 836, 1205 and 1463 kPa, respectively (Figure 5). As seen, for a drilled shaft with a diameter of 80 cm, by increasing the embedment depth from 5 m to 10 m, the amount of increase in the end bearing capacity is 44%, but by increasing the embedment depth from 10 m to 15 m, the rate of increase in the end bearing capacity is only 21%. Similar results were obtained for drilled shafts with constant diameters of 40 cm and 60 cm and different embedment depths of 5, 10 and 15 m as can be observed in Figure 5. It can be concluded that with the increase in pile embedment depth for a constant pile diameter, the end bearing capacity also increases, but with a smaller rate.

Effect of Pile Diameter

In order to investigate the influence of pile diameter on the end bearing capacity, some numerical analyses were carried out for drilled shafts with constant embedment depths of 5, 10 and 15 m and different diameters of 40, 60 and 80 cm. Figure 6 shows the variations of stresses at the pile tip *versus* pile diameter.

It is seen that the end bearing capacity for a 5-m drilled shaft with a diameter of 40 cm is 679 kPa, while this value is 768 kPa for a drilled shaft with a diameter of 60 cm and, as previously calculated, the end bearing capacity for a drilled shaft with a diameter of 80 cm is 836 kPa. In other words, by increasing the pile diameter from 40 cm to 60 cm, the rate of increase in the end bearing capacity is 13%, but by increasing the pile diameter from 60 cm to 80 cm, the amount of increase in the end bearing capacity is only 8%. Hence, for a constant embedment depth, the increase in pile diameter leads to an increase in the end bearing capacity. However, the end bearing capacity increases with a decreasing rate. Similar curves were obtained for drilled shafts with constant embedment depths of 10 m and 15m and different diameters of 40, 60 and 80 cm. It should be noted that, in Figure 6, L is the embedment depth of the drilled shaft.

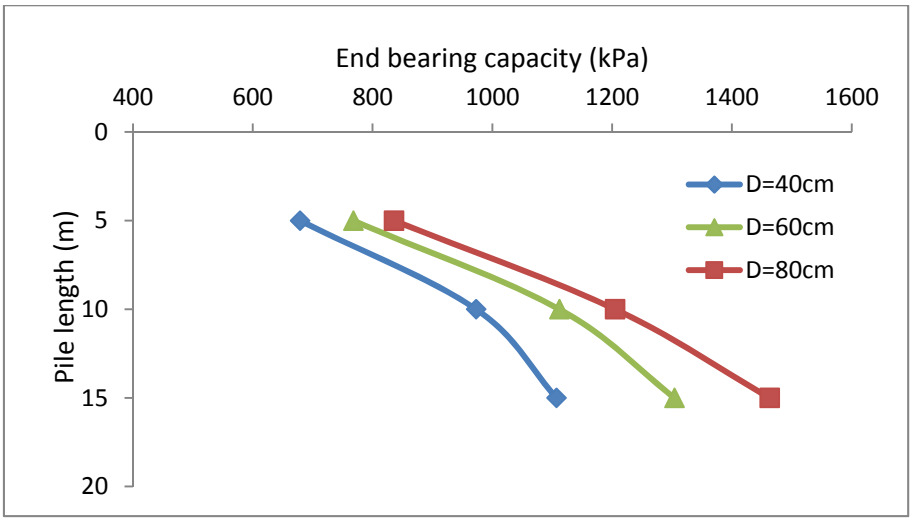

Figure (5): Variation of the end bearing capacity of drilled shafts with embedment depth

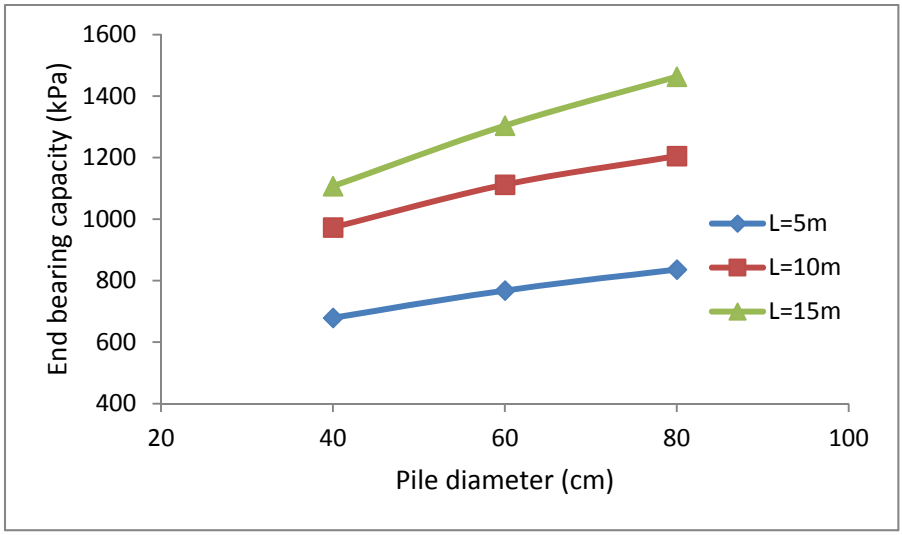

Figure (6): Variation of the end bearing capacity of drilled shafts with diameter

Table 2. Exploratory boring log

Depth (m)	Soil classification	Graphic log	N	G_S	γ (gr/cm^3)
1.0	SP		11	2.81	1.83
2.0	SP		13	2.81	1.89
3.0					
3.5	SP		15	2.79	1.88
4.0					
5.0	SP		18	2.76	1.93
6.0					
7.0					
7.5	CL		10	2.72	1.75
8.0					
9.0					
10.0	SP		25	2.81	1.98
11.0					
12.0					
12.5	CH		12	2.36	1.75
13.0					
14.0					
15.0					
16.0					
17.0					
17.5	SP		47	2.75	2.11
18.0					
19.0					
20.0	SP		50	2.75	2.12

Comparison of Ultimate End Bearing Capacity of Drilled Shafts

Drilled shafts are classified in this section in order to handle them more conveniently. This classification is shown in Table 3. Figure 7 demonstrates the ultimate end bearing capacity of drilled shafts. As expected, A1 has the lowest value and C3 has the highest value of end bearing capacity. It is seen that the end bearing capacity of B2 (D = 60 cm, L = 10 m) is a little more than the end bearing capacity of A3 (D = 40 cm, L = 15 m). This shows that with the increase in pile diameter from 40 cm to 60 cm, the influence of pile diameter on the end bearing capacity is more than that of the pile length, but this trend is not observed with the increase in pile diameter from 60 cm to 80 cm, so that the end bearing capacity of B3 (D = 60 cm, L = 15 m) is more than that of C2 (D = 80 cm, L = 10 m). Therefore, the effect of length on the value of the end bearing capacity of these piles is more significant.

Table 3. Classification of drilled shafts

Name of drilled shaft	Diameter (cm)	Embedment depth (m)
A1	40	5
A2	40	10
A3	40	15
B1	60	5
B2	60	10
B3	60	15
C1	80	5
C2	80	10
C3	80	15

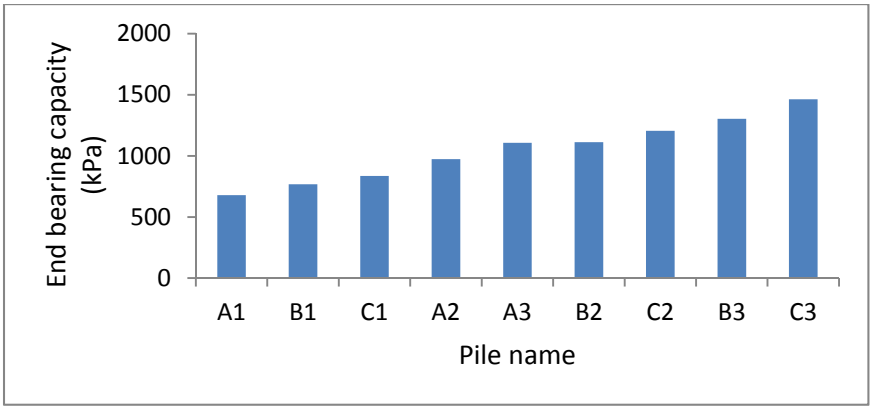

Figure (7): End bearing capacity of drilled shafts

Failure Zone around the Tip of Drilled Shafts

Figure 8 depicts numerical prediction of failure zone around the tip of a 5-m drilled shaft having a diameter of 80 cm embedded in the mentioned site in Babolsar. Meyerhof (1951) and De Beer (1963) assumed that the shape of the failure zone is logarithmic spiral and showed that the rupture surfaces extend to the body of the pile at some distance above its tip. In other words, the major part of the failure zone extends more above the pile tip, according to their recommendations. However, as observed in Figure 8, the height of the failure zone below the pile tip is more than its height above the pile tip, so that the length of the failure zone below the pile tip is 3 m and the length of the failure zone above the pile tip is 1.4 m. This difference between the results of numerically obtained analyses in this study and empirical suggestions, is related to the mechanism of shear failure. Meyerhof (1951) and De Beer (1963) assumed that the general shear failure occurs around the pile tip, while in the numerical analyses performed in this study, it is assumed that punching shear failure pattern takes place surrounding the pile tip. Similar numerical analyses were carried out on drilled shafts with a diameter of 80 cm and embedment depths of 10 m and 15 m. As depicted in Figure 9, the influence zone surrounding the tip of a pile with an embedment depth of 15 m is smaller than that surrounding the tip of a pile with an embedment depth of 10 m. Table 4 shows the length of the failure zone below and above the tip of piles. As seen, with the increase in the diameter of drilled shafts for a constant embedment depth, the length of the failure zone increases. However, with the increase in the embedment depth of piles for a constant diameter, the range of failure zone decreases. Therefore, A3 has the smallest and C1 has the largest failure zone.

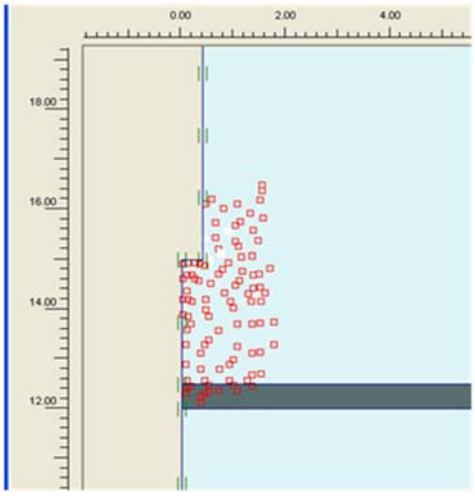

Figure (8): Numerical failure zone around the pile tip

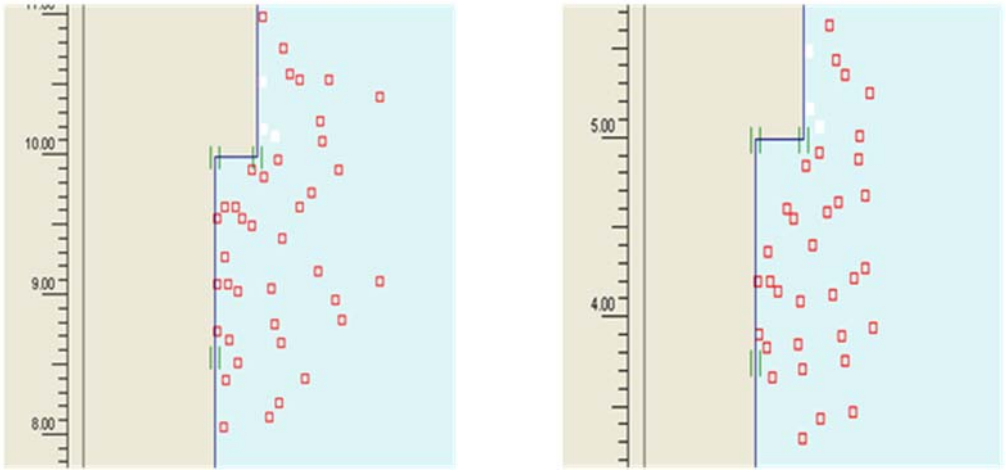

(a) (b)

Figure (9): Numerical failure zone around the tip of a pile with a diameter of 80 cm, (a) embedment depth= 10 m; (b) embedment depth = 15 m

Table 4. Length of failure zone

Name of drilled shaft	Length of failure zone (m)	
	Below pile tip	Above pile tip
A1	1.4	0.6
A2	1.0	0.4
A3	0.8	0.3
B1	2.0	1.2
B2	1.5	0.7
B3	1.2	0.6
C1	3.0	1.4
C2	2.0	1.0
C3	1.7	0.7

CONCLUSIONS

Determining the end bearing capacity of piles is an interesting issue in geotechnical engineering. In the present study, a numerical modeling procedure was applied to analyze the end bearing capacity of drilled shafts in sandy soils. The elasto-plastic Mohr–Coulomb model was used in the procedure. A comparison between numerical and measured results of pile load test showed that the agreement between results was acceptable. Numerical analyses were carried out on drilled shafts with different diameters and embedment depths. The results show that with the increase in the pile embedment depth, the end bearing capacity increases with a decreasing rate. In addition, by increasing the pile diameter, the end bearing capacity increases. However, the rate of increase becomes smaller. Based on the obtained numerical length of the failure zone above and below the tip of piles, the end bearing capacity of piles is more dependent on the properties of the soil located below the pile tip in comparison with those of the soil located above the pile tip. The results show that the failure zone around the tip of a long pile is generally smaller than that surrounding the tip of a short pile. Moreover, with the increase in pile diameter for a constant embedment depth, the range of failure zone increases.

REFERENCES

Abdrabbo, F.M., and Gaaver, K.E. (2013)."Undrained behavior of auger cast-in-place piles in multi-layered soil." Alexandria Engineering Journal, 52 (2), 187-195.

Ai, Z.Y., and Cheng, Y.C. (2013). "Analysis of vertically loaded piles in multi-layered transversely isotropic soils by BEM." Engineering Analysis with Boundary Elements, 37 (2), 327-335.

Alkroosh, I., and Nikraz, H. (2012). "Predicting axial capacity of driven piles in cohesive soils using intelligent computing." Engineering Applications of Artificial Intelligence, 25 (3), 618-627.

Brown, D.A., Turner, J.P., and Castelli, R.J. (2010). “Drilled shafts: construction procedures and LFRD design methods”. Report No. FHWA NHI-10-016, Federal Highway Administration, USA.

Chen, Y.J., and Fang, Y.C. (2009). "Critical evaluation of compression interpretation criteria for drilled shafts." Journal of Geotechnical and Geoenvironmental Engineering, 135 (8), 1056-1069.

Coduto, D.P. (2001). “Foundation design: principles and practices”. 2nd Edition, Prentice-Hall, Inc., New Jersey, USA.

DeBeer, E.E. (1963). "The scale effect in the transposition of the results of deep sounding tests on the bearing capacity of piles and caisson foundations". Geotechnique, 13 (1), 39-75.

Dung, N.T., Chung, S.G., Kim, S.R., and Beak, S.H. (2011). "Applicability of SPT-based methods for estimating toe bearing capacity of driven PHC piles in thick deltaic deposits." KSCE Journal of Civil Engineering, 15 (6), 1023-1031.

Dung, N.T., Chung, S.G., Kim, S.R., and Chung, J.G. (2007). "Comparative study between design methods and pile load tests for bearing capacity of driven PHC piles in the Nakdong river delta". Journal of the Korean Geotechnical Society, 23 (3), 61-75.

Fleming, W.G.K., Weltman, A.J., Randolph, M.F., and Elson, W.K. (1985). “Piling Engineering”. Wiley, New York, USA.

Ghashghaee Zadeh, N., and Kalantari, B. (2011). "Performance of single pile under vertical and lateral loads in sand, clay and layered soil". Electronic Journal of Geotechnical Engineering, 16 (K), 1131-1146.

Gunaratne, M. (2006). “The foundation engineering handbook”. Taylor and Francis, London.

Ishihara, K. (2010). "Recent advances in pile testing and diaphragm wall construction in Japan." Geotechnical Engineering Journal of the SEAGS and AGSSEA, 41 (3), 1-43.

Kameswara Rao, N.S.V. (2011). "Foundation design: theory and practice". 1st Edition, John Wiley & Sons, USA.

Manandhar, S., and Yasufuku, N. (2012). "Analytical model for the end-bearing capacity of tapered piles using cavity expansion theory." Advances in Civil Engineering, 2012, 1-9.

Mayne, P.W., and Harris, D.E. (1993). "Axial load-displacement behavior of drilled shaft foundations in piedmont residuum". FHWA Reference No. 41-30-2175, Georgia Tech. Research Corporation, USA.

Meyerhof, G.G. (1951). "The bearing capacity of foundations". Geotechnique, 2 (4), 301-332.

O'Neill, M.W., and Reese, L.C. (1999). "Drilled shafts: construction procedures and design methods". Report No. FHWA-IF-99-025, Federal Highway Administration, USA.

Reese, L.C., and Wright, S.J. (1977). "Construction procedure and design for axial loading, drilled shaft manual". HDV–22, Implementation Package 77–21, Vol. 1, Implementation Division, US Department of Transportation, McLean, USA.

Tomlinson, M.J. (1994). "Pile design and construction practice". 4th Edition, E & FN SPON, London.

Veiskarami, M., Eslami, A., and Kumar, J. (2011). "End-bearing capacity of driven piles in sand using the stress characteristics method: analysis and implementation". Canadian Geotechnical Journal, 48 (10), 1570-1586.

White, D.J., and Bolton, M.D. (2005). "Comparing CPT and pile base resistance in sand". Geotechnical Engineering, 158 (1), 3-14.

Winterkorn, H.F., and Fang, H.Y. (1975). "Foundation engineering handbook". Van Nostrand Reinhold Company, Inc., New York, USA.

Yu, F., and Yang, J. (2012). "Base capacity of open-ended steel pipe piles in sand". Journal of Geotechnical and Geoenvironmental Engineering, 138 (9), 1116-1128.